

Study on Thévenin Equivalent Circuit Modeling of Zinc-Nickel Single-Flow Battery

Shouguang Yao^{1,*}, PengLiao¹, Min Xiao¹, Jie Cheng², Liang Xu²

¹ Jiangsu University of Science and Technology, Zhenjiang, 212003, China

² Zhangjiagang Smartgrid Fanghua Electrical Energy Storage Research Institute Co., Ltd, Zhangjiagang, 215600, China

*E-mail: zjyaosg@126.com

Received: 17 January 2017 / Accepted: 13 March 2018 / Published: 10 April 2017

Based on the working principle of a zinc–nickel single-flow battery (ZNB), an improved Thévenin equivalent circuit model is proposed in this paper. According to the experimental data of a 100-A pulsed discharge of a ZNB, the parameters of the modified model were obtained based on the parameter identification principle and the least squares curve fitting method first, then the discrete mathematical models of the model voltages were built in a MATLAB/Simulink environment. The simulation results show that the stack voltage's maximum relative error for the Thévenin model is 5.2% when compared with the experimental results under a 100-A constant-current discharge; the corresponding value of the improved model is 2.38%, and the relative error of the improved model is lower than that of the Thévenin model over the entire discharge process, which indicates that the improved model has higher accuracy and a more accurate prediction of the stack voltage for the battery constant-current discharge.

Keywords: zinc-nickel single-flow battery; Thévenin model; discrete mathematical model; parameter identification; model simulation

1. INTRODUCTION

Energy storage batteries play an important role in the use of renewable energy. The most significant feature of the flow battery, which distinguishes it from the traditional energy storage batteries (such as lead-acid batteries and lithium-ion batteries), is that the active substance exists in the electrolyte, so its output power and capacity are independent of each other and the system design is flexible [1, 2]. The vanadium redox flow battery (VRB) avoids the problem of capacity loss caused by electrolyte cross-contamination by its use of single-element vanadium, but the use of an ion-exchange

membrane increases the manufacturing cost of the VRB [3, 4]. The zinc-nickel single-flow battery proposed in recent years is a kind of cost-effective energy storage device, which is an important power storage component in the field of smart grids, renewable energy, and distributed power supply. The zinc-nickel single-flow battery uses a single electrolyte and no ion exchange membrane, and has the advantages of a simple structure, long cycle life, high reliability, and no pollution [5-8]. The zinc-nickel single-flow battery is widely used, and imposes higher requirements on intelligent management systems for energy storage; to estimate and predict the battery performance states scientifically and accurately to maximize the ZNB discharge power and ensure stable, long-term, reliable performance, there is a need to build an accurate, convenient, and common model [9, 10].

Applying the model to energy storage systems not only considers the accuracy of the model to restore the working state of the battery as much as possible, but also considers the simplicity of the model to improve computational efficiency. At present, the methods for battery modeling are the electrochemical mechanism model and the equivalent circuit model [11, 12]. The electrochemical mechanism model describes a complicated physical and chemical process inside the battery; thus, it is rarely used for actual systems because of its complicated form and time-consuming calculation. The equivalent circuit model is composed of ideal circuit elements (such as resistors, capacitors, and controllable voltage sources), and uses linear parameter varying (LPV) to simulate the non-linear characteristics of the battery. Thus, its accuracy is slightly worse than that of the electrochemical model, but it has been widely used because of its advantages of linear characteristics, easy calculation, and suitability for real-time systems. Commonly used equivalent circuit models include the Rint model, PNGV model, GNL model, and Thévenin model [13-15]. Now the research on the ZNB modeling is mainly focused on the electrochemical modeling, and the equivalent circuit modeling of the ZNB is rarely studied. Therefore, the purpose of this paper is to propose an equivalent circuit model suitable for the ZNB. Among the equivalent circuit models, Thévenin model is the most widely used model, which can simulate the dynamic and static characteristics of the battery and charge-discharge characteristics well with good dynamic adaptability, and it's easy to achieve parameter identification with high precision due to relatively simple structure [16].

In this study, an improved model of ZNB was established on the basis of the Thévenin model. The model parameters were obtained by an impulse experiment, and discrete mathematical models of the voltage in the improved model were obtained by means of discretization. The results show that the improved model is more suitable than the Thévenin model for ZNB equivalent circuit modeling, thus providing a reference for future ZNB energy storage.

2. EXPERIMENTAL

2.1. ZNB Working Principle

The positive electrode of a ZNB is made of nickel oxide, the electrolyte is an alkaline solution of high-concentration zincate, and an inert current collector is used as the negative electrode of the battery. During charge and discharge, the electrolyte is circulated by the pump, as shown in Figure 1.

During discharge, the zinc is oxidized to zincate on the negative electrode substrate, losing electrons to the positive electrode, and $NiOOH$ is reduced to $Ni(OH)_2$ at the positive electrode. When the battery is charged, the reaction becomes the reverse of the discharge reaction.

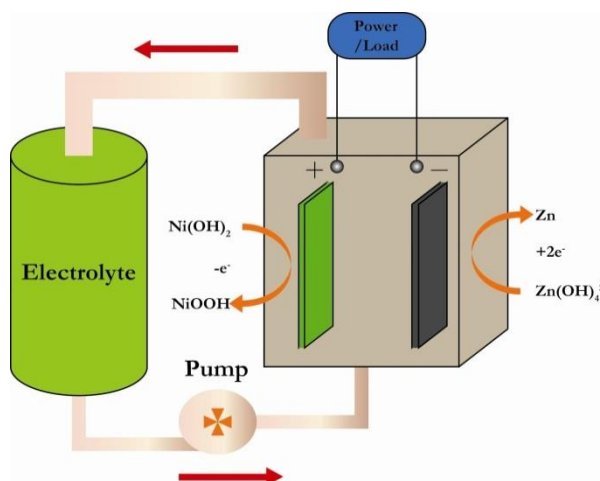


Figure 1. Zinc–nickel single-flow battery working principle.

2.2. ZNB State of Charge

The state of charge SOC of the battery indicates the ratio of the capacity remaining to the nominal capacity; SOC equals 1 when the battery is fully charged, and SOC equals 0 when the battery is discharged completely [17]. Because the estimation of the battery SOC is the most important part of the battery intelligent management system, this study investigated only the dynamic change of the stack voltage under the ZNB constant-current discharge condition, and thus adopted the simple and convenient ampere-hour integral method to estimate SOC [18]. In this study, the discharge current direction is set to be positive; using the battery discharge process as an example, the estimated discrete formula of SOC is

$$SOC(k+1) = SOC(k) - \frac{\eta \Delta t I_L(k)}{Q_N} \quad (1)$$

where $SOC(k)$ is the value of SOC at time k ; η is the charge-discharge efficiency of the battery, which is a variable in theory, and set to $\eta=0.94$ here; Δt is the sampling period; $I_L(k)$ is the value of current at time k ; and Q_N is the rated capacity of the battery.

2.3. ZNB Equivalent Circuit Model

In general, the following points are necessary for a good model: 1) the model can accurately describe the dynamic and static characteristics of the battery; 2) the model itself is less complex and easy to calculate; and 3) the project implementation is relatively simple and feasible. Based on these points, this paper proposes an improved Thévenin model (see Figure 2) that is suitable for ZNB. The

improved model adds an RC circuit on the basis of the Thévenin model (see Figure 3). Figure 4 shows the response curve of the ZNB stack voltage of one certain discharge pulse.

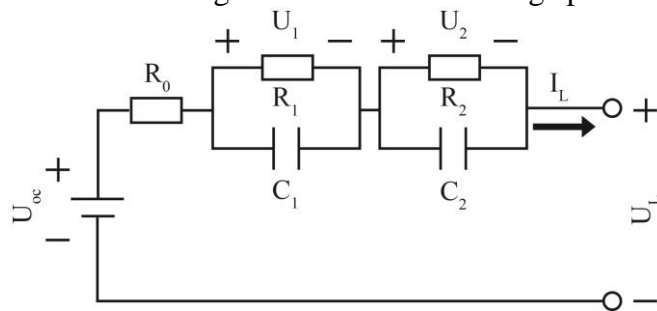


Figure 2. Improved ZNB model.

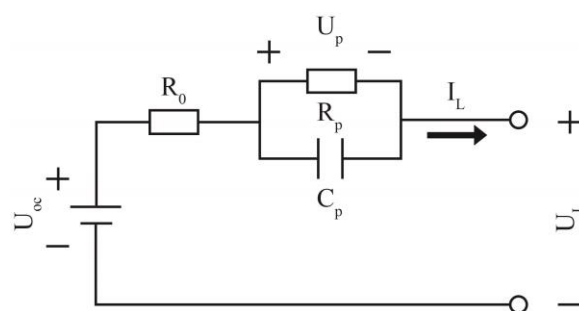


Figure 3. Thévenin model of a ZNB.

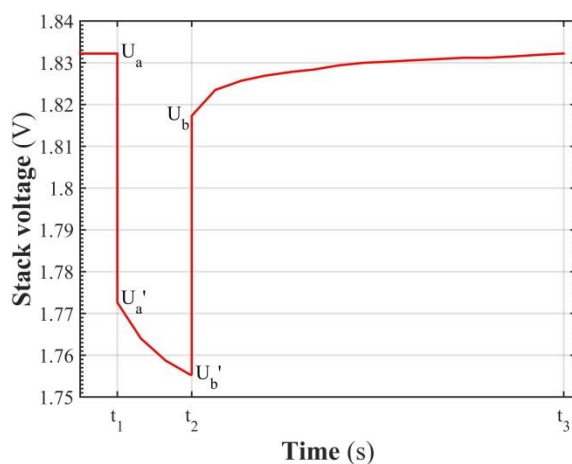


Figure 4. Response curve of the ZNB stack voltage for one certain discharge pulse.

Aiming at an improved ZNB model, the equivalent process of the model is briefly analyzed according to the response curve of the stack voltage for one certain pulse. As shown in Figure 4, when loading a current (at time t_1) or canceling the current (at time t_2) only, the value of the stack voltage has a transition (drops from U_a to U_a' , or rises from U_b to U_b'), which is similar to the voltage response of applying a current to a pure resistance, namely corresponding to the ohmic resistance R_0 in

the model. The two section curves of the voltage changing slowly in Figure 4 can be described by the serial RC circuits: R_1 and C_1 are used to describe the ZNB's concentration polarization phenomenon, which is a process of discharge voltage U_1 to be slow and stable with a large time constant; R_2 and C_2 are used to describe the ZNB's electrochemical polarization phenomenon, which is a process of discharge voltage U_2 to be a quick change with a small time constant. U_{oc} in the model indicates the open-circuit voltage of the battery, which has a fixed-function relation with the battery SOC in certain cases. In general, the concentration polarization of ZNB (including the solution concentration polarization and proton concentration polarization in the positive solid phase) has a great influence, followed by ohmic polarization and electrochemical polarization [19].

According to the equivalent circuit model diagram and Kirchhoff circuit theorem, and with the discharge current direction set as the positive direction of current, the mathematical relationship of the improved model parameters can be obtained.

$$U_L = U_{oc} - U_1 - U_2 - R_0 I_L \tag{2}$$

$$\dot{U}_1 = -\frac{U_1}{C_1 R_1} + \frac{I_L}{C_1} \tag{3}$$

$$\dot{U}_2 = -\frac{U_2}{C_2 R_2} + \frac{I_L}{C_2} \tag{4}$$

2.4. Model Parameter Identification

The ZNB electrochemical process is highly complex during charging and discharging, and the ZNB characteristics are nonlinear and time varying. It is highly difficult to obtain the parameters in the model by theoretical analysis. Therefore, it is necessary to conduct an analysis of the experimental curve; that is, using the current input and voltage output of the case, to calculate the various parameters of the battery model, according to which the current state of the battery is estimated in order to achieve better management of the battery [20].

For the improved model as shown in Figure 4, with a canceled pulse current (i.e., $I_L(t) = 0$), the stack voltage of the battery is equal to the sum of the open-circuit voltage U_{oc} and the voltage drop of the two serial RC circuits. During the idle time, the charge in capacitors C_1 and C_2 discharge the resistances R_1 and R_2 , respectively, through the RC circuits and disappear gradually; then, the stack voltage is approximately equal to the open-circuit voltage. After the current was canceled, the shape of the stack voltage curve changing slowly was presented as the shape of the exponential function, and the curve was similar to the zero-input response of the RC circuit, which could be described by

$$U_{sum} = U_1 + U_2 = U_{10} e^{-t/\tau_1} + U_{20} e^{-t/\tau_2} \tag{5}$$

where the RC circuit time constants are $\tau_1 = R_1 C_1$ and $\tau_2 = R_2 C_2$, U_{10} and U_{20} are the initial voltage across the capacitor, and t is the time.

Through Equations (2) and (5), the equation of the stack voltage curve can be expressed as

$$U_L(t) = U_{oc} - U_1 - U_2 = U_{oc} - U_{10} e^{-t/\tau_1} - U_{20} e^{-t/\tau_2} \tag{6}$$

With the actual response value and the expression of the stack voltage, the undetermined coefficients (i.e., U_{10} , U_{20} , τ_1 and τ_2 in Equation (6)) can be calculated by using the least squares curve fitting technique.

When loading current, the stack voltage decreasing slowly as shown in Figure 4 can be seen as the sum of the open-circuit voltage U_{oc} and the voltage drop of the two serial RC circuits. Similarly, after loading the current, the shape of the stack voltage curve changing slowly is also presented as the shape of the exponential function, and the curve is similar to the zero-state response of the RC circuit, which is described by

$$U_{sum} = U_1 + U_2 = IR_1(1 - e^{-t/\tau_1}) + IR_2(1 - e^{-t/\tau_2}) \quad (7)$$

Through Equations (2) and (7), the equation of the stack voltage curve can be expressed as

$$U_L(t) = U_0 - U_1 - U_2 = U_0 - IR_1(1 - e^{-t/\tau_1}) - IR_2(1 - e^{-t/\tau_2}) \quad (8)$$

where U_0 is the voltage at the beginning of discharge.

The values of τ_1 and τ_2 calculated previously are substituted into Equation (8). Similarly, with the actual response value and the expression of the stack voltage, the values of R_1 and R_2 can be calculated by using the least squares curve fitting technique. The value of R_0 is calculated only by dividing the sudden-change value of stack voltage (shown in Figure 4) by the discharge current:

$$R_0 = \frac{U_a - U_a'}{I_L} = \frac{U_b' - U_b}{I_L} \quad (9)$$

2.5. Experimental Test

The ZNB model parameters change with changing operating conditions. If the parameters under one certain pulse are used only for simulation, the accuracy of the model will be greatly reduced. In order to accurately identify the value of the ZNB model parameters during the whole discharge and to verify the improved model, the following experiments were designed in this study:

Pulse experiments:

1) Idle the fully charged battery for 10 min, then collect the data of the stack voltage; 2) discharge the battery for 1 minute with a constant 100-A current, and collect the stack voltage data; 3) idle the battery for 5 min, and collect the stack voltage data; and 4) repeat steps 2) and 3) until the battery reaches the cut-off voltage.

Constant-current discharge test:

Discharge the fully charged battery with a constant 100-A current until the battery reaches the cut-off voltage.

The nominal voltage of the ZNB tested in this study was 1.6 V, the rated capacity was 300 Ah, the cut-off voltage of charge was 2.1 V, the cut-off voltage of discharge was 1.2 V, and the pulse current was 100 A. The experiments were carried out at room temperature (25 °C).

3. RESULTS AND DISCUSSION

3.1. Identification Results

According to the principles and calculation formulas described previously, the open-circuit voltage, ohmic resistance, electrochemical polarization resistance, concentration polarization

resistance, and time constants of a ZNB under a 100-A constant-current pulse discharge condition can be calculated; the relationship curves between them and SOC are shown in Figure 5.

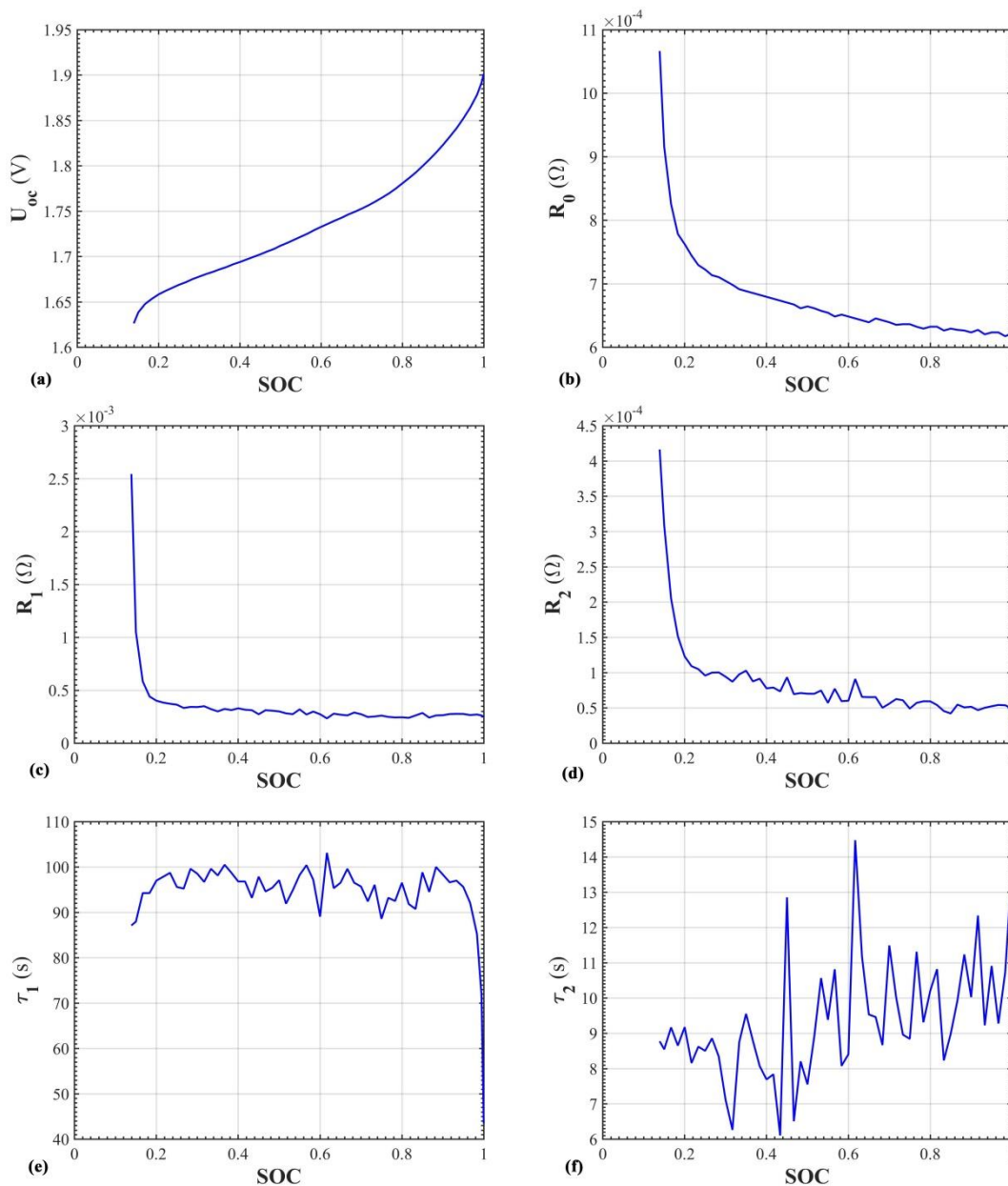


Figure 5. Parameters of the ZNB improved model changing with SOC .

As shown in Figure 5(a), the open-circuit voltage U_{oc} increases almost linearly with increasing SOC when $0.2 < SOC < 0.8$, and the change accelerates when $SOC < 0.2$ or $SOC > 0.8$ and is especially more significant when $SOC < 0.2$. As shown in Figure 5(b), the internal resistance R_0 of the battery decreases slowly with increasing SOC when $SOC > 0.2$; the internal resistance increases significantly with decreasing SOC when $SOC < 0.2$, because the conductivity of the cathode activity is substantially reduced under low-power conditions [21, 22]. The variation trend of the concentration polarization resistance R_1 (see Figure 5(c)) or the electrochemical polarization resistance R_2 (see Figure 5(d)) is consistent with the internal resistance of the battery; the value of R_1 or R_2 presents a

fluctuated slowly decreasing trend, and the value of R_2 is smaller than that of R_1 by an order of magnitude. Comparing the internal resistance, concentration polarization resistance, and electrochemical polarization resistance reveals that the concentration polarization loss is the key factor determining the battery discharge characteristics, the ohmic internal resistance has a great influence on the curve at the end of discharge, and the chemical polarization loss has the smallest effect on the battery discharge curve [19]. As shown in Figure 5(e), the time constant of the concentration polarization τ_1 is in the process of fluctuating, and is essentially maintained between 90 s and 100 s; τ_1 sharply decreases with increasing SOC, which is caused by the significant change of the concentration polarization at the beginning of discharge [5, 6]. Compared with τ_1 , the electrochemical polarization time constant τ_2 fluctuates more drastically and is smaller than τ_1 numerically by an order of magnitude overall.

The above-mentioned principle of parameter identification of the improved ZNB model and the analysis of the variation of the model parameters are also applicable to the Thévenin model, so they are not reiterated here.

3.2. Simulation Results

The battery equivalent circuit model in practice is in discrete form, so the improved ZNB model is discretized as follows:

$$U_L(k) = U_{oc} - U_1(k) - U_2(k) - R_0 I_L(k) \quad (10)$$

$$U_1(k+1) = U_1(k)e^{-\Delta t/\tau_1} + I_L(k)R_1(1 - e^{-\Delta t/\tau_1}) \quad (11)$$

$$U_2(k+1) = U_2(k)e^{-\Delta t/\tau_2} + I_L(k)R_2(1 - e^{-\Delta t/\tau_2}) \quad (12)$$

where k is the random sampling point in the ZNB simulation process, and Δt is the sampling period in the simulation process. Through previous calculation and the formulas, the improved model is shown in Figure 6.

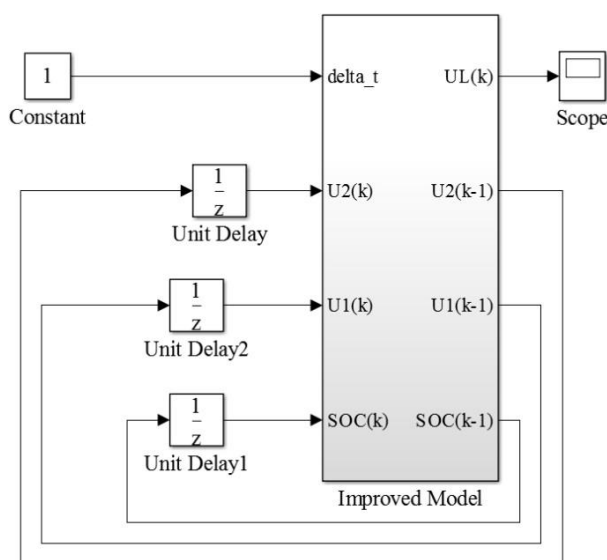


Figure 6. Simulation chart of the improved ZNB model.

The discretization process of the voltage expression of the improved ZNB model and the modeling process are also applicable to the Thévenin model, so they are not reiterated.

In this study, the 100 A constant-current discharge is taken as an example to compare the simulation curves of stack voltage of the Thévenin model and the improved model with an experimental curve to determine the accuracy and error of the two kinds of ZNB models. Figure 7 shows the comparison results of the stack voltage of the two kinds of models compared with the experimental curve. Figure 8 shows the relative error curves of the two kinds of models.

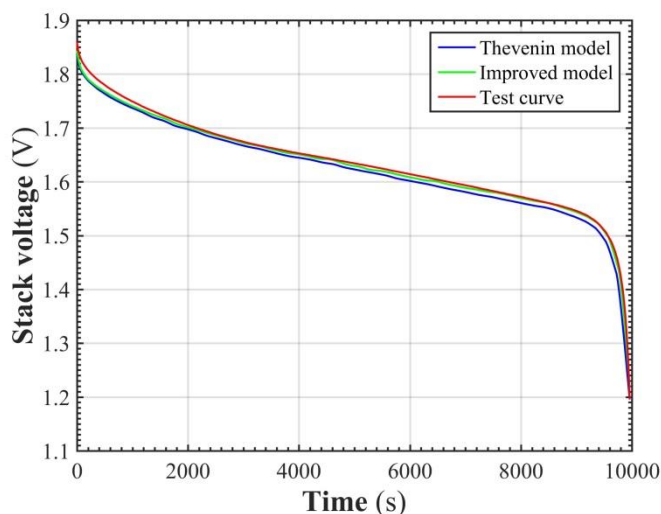


Figure 7. Comparison of stack voltage curves between the two kinds of models and experimental result.

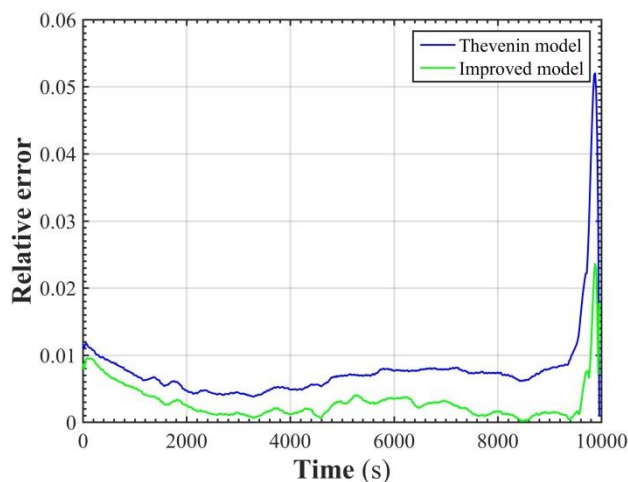


Figure 8. Comparison of relative error curves of stack voltage between the two kinds of models.

As shown in Figure 7, the simulation curve of stack voltage of the ZNB Thévenin model is similar to the experimental curve in shape, but it can be seen that the fitting degree of the two curves is not ideal. However, the stack voltage curve of the improved model has a higher degree, which can describe the ZNB discharge response more accurately. At the same time, the relative error of stack

voltage of the two models is relatively large at the beginning or end of battery discharge, which may be due to the short idle time set in the pulse test [20]. As shown in Figure 8, the maximum relative error between the voltage value of the Thévenin model and the experimental value is 5.2%, whereas the maximum relative error of the improved model is 2.38%, and the relative error of the stack voltage of the improved model is lower than that of the Thévenin model, indicating that the accuracy of the improved model is higher and the prediction of stack voltage under constant-current discharge is more accurate. In summary, the improved model can be used to characterize the ZNB stack voltage.

4. CONCLUSIONS

From the response curve of the ZNB pulse discharge, the circuit equivalent mechanism of the stack voltage variation was analyzed, and an improved Thévenin equivalent circuit model was established. Then, the relationships between the parameters of the improved model and *SOC* were obtained through the pulse discharge experimental data of a 300-Ah single cell, and 100-A constant-current discharge simulation models were built in a MATLAB/Simulink environment. Through the experimental and simulation analysis, the following conclusions were obtained:

1. The maximum relative error of the improved ZNB model is 2.38%, which is lower than that of the Thévenin model, indicating that the improved model has higher accuracy and is more suitable for ZNB equivalent circuit modeling research.
2. The relative error of stack voltage of the two models is large at the beginning or the end of battery discharge, and is related to the short idle time set in the pulse test.

ACKNOWLEDGEMENTS

We gratefully acknowledge the financial support of the National High Technology Research and Development Program of China (2012AA052003).

References

1. X. Sun, B. Zhang, X. Tang, B. McLellan and M. Höök, *Energies*, 9 (2016) 980.
2. Z. Yang, J. Zhang, M. C. Kintner-Meyer, X. Lu, D. Choi, J. P. Lemmon and J. Liu, *Chem rev*, 111 (2011) 3577.
3. C. Flox, M. Skoumal, J. Rubio-Garcia, T. Andreu and J. R. Morante, *Appl Energ*, 109 (2013) 344.
4. X. Zhang, Y. Li, M. Skyllas-Kazacos and J. Bao, *Energies*, 9 (2016) 857.
5. J. Cheng, Y.-H. Wen, G.-P. Cao and Y.-S. Yang, *J Power Sources*, 196 (2011) 1589.
6. J. Cheng, L. Zhang, Y.-S. Yang, Y.-H. Wen, G.-P. Cao and X.-D. Wang, *Electrochem Commun*, 9 (2007) 2639.
7. S. Yao, P. Liao, M. Xiao, J. Cheng and K. He, *AIP Adv*, 6 (2016) 125302.
8. L. Zhang, J. Cheng, Y.-s. Yang, Y.-h. Wen, X.-d. Wang and G.-p. Cao, *J Power Sources*, 179 (2008) 381.
9. H. Rahimi-eichi, U. Ojha, F. Baronti and M.-y. Chow, *IEEE IND ELECTRON M*, 13 (2013) 4.
10. S. M. Rezvanianiani, Z. Liu, Y. Chen and J. Lee, *J Power Sources*, 256 (2014) 110.
11. H. He, R. Xiong and J. Fan, *Energies*, 4 (2011) 582.

12. H.-W. He, R. Xiong and Y.-H. Chang, *Energies*, 3 (2010) 1821.
13. S. X. Chen, H. B. Gooi, N. Xia and M. Q. Wang, *IET Electrical Systems in Transportation*, 2 (2012) 202.
14. V. H. Johnson, *J Power Sources*, 110 (2002) 321.
15. Z. M. Salameh, M. A. Casacca and W. A. Lynch, *IEEE T Energ Conver*, 7 (1992) 93.
16. S. Tian, M. Hong and M. Ouyang, *IEEE T Energ Conver*, 24 (2009) 452.
17. D. Sun and X. Chen, *2014 17th International Conference on Electrical Machines and Systems (ICEMS), Hangzhou, China, 2014*, 855-860.
18. X. Hu, S. Li and H. Peng, *J Power Sources*, 198 (2012) 359.
19. J. W. Weidner and P. Timmerman, *J Electrochem Soc*, 141 (1994) 346.
20. G. L. Plett, *J Power Sources*, 134 (2004) 262.
21. W. B. Gu, C. Y. Wang, S. M. Li, M. M. Geng and B. Y. Liaw, *Electrochim Acta*, 44 (1999) 4525.
22. P. D. Vidts, J. Delgado and R. E. White, *J Electrochem Soc*, 143 (1996) 3223.

© 2018 The Authors. Published by ESG (www.electrochemsci.org). This article is an open access article distributed under the terms and conditions of the Creative Commons Attribution license (<http://creativecommons.org/licenses/by/4.0/>).